Chemical Engineering Journal xxx (xxxx) 143509

Contents lists available at ScienceDirect

Chemical Engineering Journal

journal homepage: www.elsevier.com/locate/cej

Assessing the feasibility of a downstream heterogeneous Fenton process for the oxidative degradation of biologically treated ranitidine, diclofenac, and simvastatin

Thiago H.G. da Silva, Rafaely X. de S. Furtado, Marcelo Zaiat, Eduardo B. Azevedo *

São Carlos Institute of Chemistry, University of São Paulo, C.P.780, São Carlos, SP CEP 13560-970, Brazil

ARTICLE INFO

Keywords:
Ranitidine
Diclofenac
Simvastatin
Anaerobic-aerobic digestion
Heterogeneous Fenton

ABSTRACT

This work assesses the feasibility of coupling the heterogeneous Fenton process to biologically treated domestic sewage to remove diclofenac, ranitidine, and simvastatin (50 μg L^{-1} each). The catalyst was a purified natural zeolite, which was impregnated with iron (2Fe4A). First, batch tests (10 g L^{-1} catalyst, 2 g L^{-1} H_2O_2, and pH 7) were performed to gather information about the performance of the process. Simvastatin could not be significantly removed as its molecular dimensions were larger than the zeolite pores. Drugs removal by adsorption and mineralization were not observed. After five cycles of 30 h each, leached iron was approximately 2%, with no significant change in the drugs removal performance. Second, a fixed-bed reactor packed with 2Fe4A was placed after the exit of the biological reactor, with hydraulic retention time of 12 min. 98 and 82% of diclofenac and ranitidine, respectively, were removed, as well as 93% of the added hydrogen peroxide. The coupled system was stable for, at least, 10 days. The operating cost of the heterogeneous Fenton process combined to the biological one was estimated and, although diclofenac and ranitidine could be significantly removed in a short period of time, it was concluded that it is a relatively expensive process that has the disadvantages of high hydrogen peroxide consumption and size exclusion effects.

1. Introduction

There is an ever-growing concern regarding the fate of organic, synthetic chemicals like pharmaceuticals, as they are emerging pollutants frequently worldwide detected in surface waters at quite low concentrations (ng L^{-1} to μg L^{-1}) [1–4].

Diclofenac (DCF), ranitidine (RNT), and simvastatin (SVT) are three important examples of pharmaceuticals/emerging pollutants found in the environment. DCF is an analgesic, antipyretic, non-steroidal anti-inflammatory drug (NSAID) used for painkilling. High doses of DCF can cause serious health problems, such as stroke and damage to the liver and kidneys [5,6]. RNT is commonly used against peptic ulcer and gastroesophageal reflux disease [7,8]. SVT has an antihyperlipidemic activity, which reduces cholesterol levels by inhibiting the HMG-CoA reductase, besides being used in the treatment of brain diseases and different types of cancer [9–11]. In wastewaters, DCF [12], RNT [13], and SVT [14] are reported to reach concentrations up to 200, 160, and 12 μg L^{-1}, respectively.

The presence of pharmaceuticals in the environment represents a potential risk to the health of living beings, as they may be carcinogenic, mutagenic, and capable of affecting the endocrine system of some aquatic organisms [15,16]. Some of them do not exert direct ecotoxicity; however, they may induce bacterial resistance and synergism with other drugs is always a possibility [7].

Wastewater treatment plants (WWTP) are one of the main sources of pharmaceutical drugs in the environment [2,17]. Therefore, it is necessary to develop sewage treatment processes capable of efficiently removing those contaminants, even in low concentrations. However, it is risky to rely on conventional processes only, considering a scenario in which several contaminants have been identified in water bodies, and the rapid growth of the world population and industrial activities [18].

Conventional effluent treatment processes were established many decades ago, when it was mainly necessary to remove organic matter. However, the effectiveness of those processes became limited since the 1970 s, when it was found that sewage, domestic, and industrial effluents might contain poorly biodegradable and/or toxic compounds [19]. Although one cannot use systems composed exclusively of biological

* Corresponding author at: Av. Trabalhador São-Carlense, 400, Parque Arnold Shimidt, São Carlos/SP, 13560-970, Brazil.
E-mail addresses: dasilvathg@iqsc.usp.br (T.H.G. da Silva), zaiat@sc.usp.br (M. Zaiat), bessa@iqsc.usp.br (E.B. Azevedo).

https://doi.org/10.1016/j.cej.2023.143509
Received 27 January 2023; Received in revised form 9 May 2023; Accepted 11 May 2023

processes to degrade those biorecalcitrant compounds, they can be coupled/combined to several other chemical processes, such as the advanced oxidation processes (AOP).

In AOPs, highly reactive species are generated, e.g., hydroxyl radical (•OH), which are capable of oxidizing a variety of substances (low selectivity); if one considers organic molecules, they may undergo mineralization (conversion into stable inorganic compounds such as CO_2, H_2O, etc.). Simultaneously, detoxification and increased biodegradability of the wastewater may happen [20–23].

Several AOPs have been used to degrade DCF, RNT, and SVT, as reported in the literature, including heterogeneous photocatalysis [24], Fenton [25], eletrochemical degradation [26], ozonation [27], electro-Fenton and solar electro-Fenton [28], heterogeneous Fenton [29], etc.

Heterogeneous Fenton processes are very popular AOPs due to their ease of operation and efficient removal of recalcitrant organic compounds, such as pharmaceuticals, from aqueous system [20,30–33].

In the heterogeneous Fenton process, the generation of •OH radicals occurs through the catalytic decomposition of H_2O_2 using iron supported in a porous material [34,35]. Several solid supports such as zeolites [8,33], activated charcoal [36], clays, and mesoporous materials [31] have been studied for the immobilization of iron. Those materials are effective for oxidizing contaminants in water because they combine high activity, recyclability, and a wide pH range for applications [8, 37].

Zeolites are stable during AOPs, making them one of the most suitable materials for the oxidation of micropollutants [38]. When added to the zeolitic channels, iron becomes stable as mono and binuclear species, which decompose hydrogen peroxide [39].

Therefore, this work first aimed at studying the degradation of a mixture of pharmaceuticals (DCF, RNT, and SVT) by combining anaerobic–aerobic and heterogeneous Fenton processes. It is important to highlight that the anaerobic–aerobic coupled degradation of DCF, RNT and SVT in domestic sewage was studied and discussed by Silva et al. (2020) [40], who observed that the DCF and SVT degradation products (DPs) were recalcitrant to the process. Moreover, as SVT and the degradation product from DCF have high lipophilicity ($\log D \geq 4.5$), they are prone to bioaccumulation. Therefore, an additional treatment process is of utmost importance for removing them as much as possible.

A low-cost material, made from natural zeolite, was synthesized, characterized, and used as a catalyst for the drugs degradation in domestic sewage. Afterwards, the heterogeneous Fenton process was used to degrade the contaminants still present in the effluent of the anaerobic–aerobic process.

2. Materials and methods

The degradation of DCF, RNT, and SVT (50 μg L^{-1} each) in domestic sewage was performed by combining the effluent of a tandem anaerobic–aerobic process, previously studied by Silva et al. [40], and the heterogeneous Fenton one.

That concentration prevented the small amounts of the target drugs already present in the sewage (approximately 100 ng L^{-1}) from significantly change the input concentrations to the reactor. Moreover, the sewage main characteristics were: 589 < COD (chemical oxygen demand) < 823 mg O_2 L^{-1}, 6.7 < pH < 6.9, 38 < TN (total nitrogen) < 40 mg L^{-1}, and 174 < TSS (total suspended solids) < 264 mg L^{-1}.

First, batch tests with the heterogeneous Fenton process were performed to know the best operational condition. Afterwards, the biological and heterogeneous Fenton processes were combined, and the cost/benefit of placing the AOP after the biological process was estimated. Fig. 1 shows a general flowchart of the steps performed throughout this study.

2.1. Heterogeneous Fenton process

2.1.1. Preparation of the catalyst

A natural zeolite (70% heulandite, 15% anorthite, 10% quartz, and 5% mordenite) from the Tijeras deposit, Vila Clara, Cuba, was the support for iron in the heterogeneous Fenton process. To remove impurities from the natural zeolite, create mesopores, and increase its hydrophobicity, the following methodology, proposed by Verboekend et al. [41],was applied: a zeolite (0.3–0.5 mm particle diameter) suspension (67 g L^{-1} in HCl 1 mol L^{-1}) was magnetically stirred and heated (100 °C) for 4 h. That procedure was repeated three times, renewing the acid solution after each cycle. Finally, the modified zeolite was washed with distilled water to constant pH (~6.5) and oven-dried at 65 °C for 24 h.

As the acid treatment removed the iron naturally present in the zeolite, it was necessary to add this element again. For that purpose, the pH of a modified zeolite suspension (100 g L^{-1}) was adjusted to 9–10 with NH_4OH 30%. Nitrogen was bubbled into the suspension to remove any

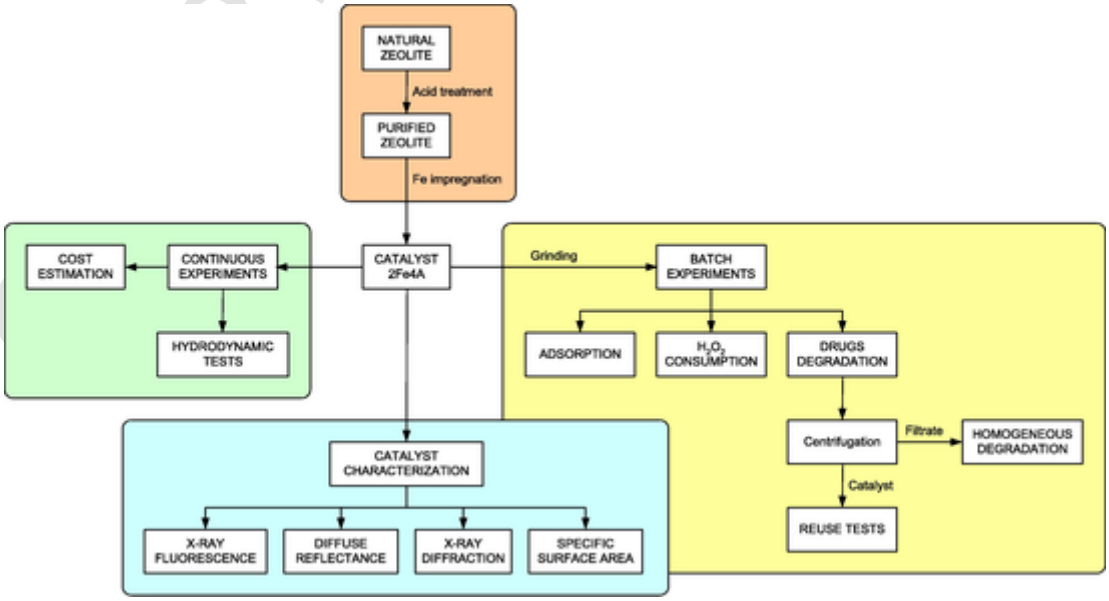

Fig. 1. General flowchart of the steps performed throughout this study.

dissolved oxygen and prevent its dissolution. The suspension was then stirred for 20 min and the pH was adjusted to 3–4 with H_2SO_4 25% (in volume). Throughout the whole process, temperature was maintained between 80 and 90 °C. Afterwards, $FeSO_4{\cdot}7H_2O$ (70 mmol L^{-1}) was added to the suspension, which was stirred for 6 h. The iron-supported zeolite was washed with distilled water 5 times, followed by washing with H_2O_2 1 g L^{-1} for oxidizing the residual Fe(II). This material was oven-dried (100 °C) for 24 h [42]. Part of this material was macerated until a diameter < 75 μm and used for the batch experiments. The remaining material (diameter between 0.3 and 0.5 mm) was used as the filling of a fixed-bed reactor.

2.1.2. Batch adsorption and degradation experiments

The adsorption and degradation of DCF, RNT, and SVT (50 μg L^{-1}, each) by the heterogeneous Fenton process were studied initially in batches during 8 h, catalyst concentration 10 g L^{-1}, 2 g L^{-1} H_2O_2, and pH 7 ± 0.2. The pH of the resulting suspension was adjusted with NaOH or HNO_3 0.1 mol L^{-1}. The adsorption equilibrium was reached after 1 h of stirring the suspension at 150 rpm and 22 ± 2 °C.

Oxidation started with the addition of H_2O_2. At the end of the reaction, an aliquot of the suspension was filtered through a 0.45 μm membrane, and the filtrate analyzed. Before the chromatographic analyses, the remaining H_2O_2 was completely degraded by adding Na_2SO_3 in a concentration two times higher than the stoichiometric ratio of the reaction·H_2O_2 and Fe concentrations were quantified by spectrophotometric methods, as described in section 2.2.

2.1.3. Hydrodynamic tests in the continuous reactor

Since the reactors were operated with continuous flow (0.7 mL min^{-1}), it was necessary to determine the average hydraulic retention time (HRT). 1 g L^{-1} NaCl was used as a tracer and conductivity was monitored at the reactor outlet every minute. The procedure was adapted from Levenspiel [43] and consisted of the following steps: 1) feeding the reactor with distilled water and flow adjustment; 2) replacing distilled water by the NaCl solution; 3) conductivity monitoring during three times the nominal HRT; 4) constructing a normalized conductivity curve (C/C_0) as a function of time; and 5) The average HRT was the time corresponding to C/C_0 = 0.5.

2.1.4. Reactors operation

The processes were combined as follows: biological process and then the heterogeneous Fenton one (Fig. 2).

Considering that this reactor had a total volume of 47.3 mL and that 38.8 g of 2Fe4A catalyst were used (specific weight 0.8 g mL^{-1}), the volume of the liquid phase was 8.5 mL and the suspension was equivalent to 4,560 g L^{-1} of solids. Sampling was always performed after a period of time equivalent to ten times the HRT, when the reactors were considered stable (see Fig. 3).

2.2. Analytical procedures

The concentrations of DCF, RNT, and SVT were quantified by SPE-HPLC-MS/MS (SILVA et al., 2020), using a liquid chromatograph (Agilent Technologies, 1200) with quaternary pump (Infinity, 1260), autosampler (Infinity, 1260), column compartment with temperature control (Infinity, 1290), diode array detector (DAD–Infinity, 1209), λ = 235 nm, and C_{18} column (Phenomenex, 3 μm, 150 × 3 mm) at 40 °C. The mobile phase was acetonitrile (ACN) and ammonium acetate 5 mmol L^{-1} 10:90 in volume. The elution gradient was (ACN): 0–5 min, 10–100%; 5–8 min, 100%; 8–10 min, 100–10%; and 10–15 min, 10%), 100 μL injection volume, 0.5 mL min^{-1} flow rate.

Q-Trap hybrid mass spectrometer (QTrap 5500, AB SCIEX) with electrospray ionization source was used to analyze the samples. Multiple reaction monitoring (MRM) was chosen for identifying and quantifying the drugs, using the following transitions of the precursor and its more abundant product ions (*m/z*): RNT–315/102, 315/130, and 315/176; DCF–296/205 and 296/214; SVT–436/285 and 436/419. Source and gas parameters used in the drugs quantification were: Gas curtain (15 psi), spray voltage (4,000 V), temperature (700 °C), heating gas (40 psi), and nebulizer gas (50 psi).

Total organic carbon analyses (TOC, Sievers InnovOx–GE) were performed to determine the mineralization degree during the degradation process.

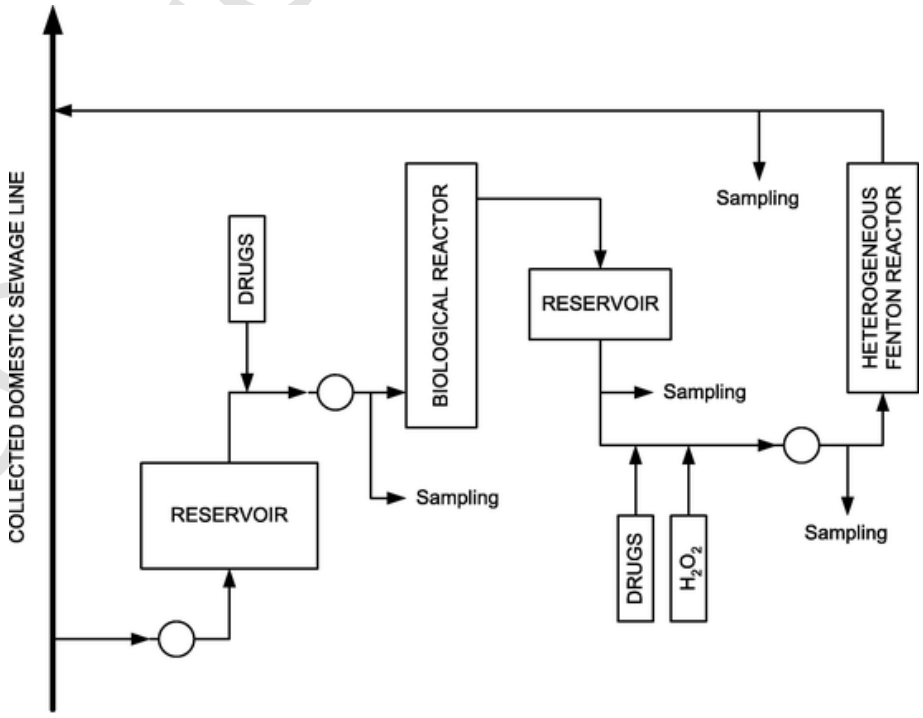

Fig. 2. Operation flowchart of the combined processes.

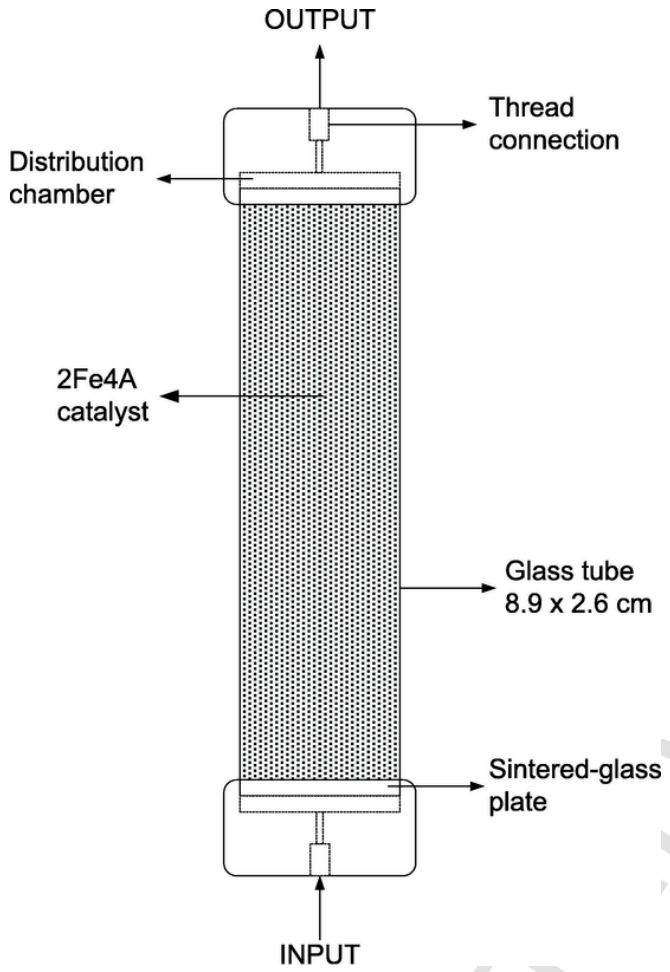

Fig. 3. Fixed-bed reactor used in the heterogeneous Fenton process.

Total iron and residual peroxide concentrations were determined by spectrophotometric methods, as described by the Standard Methods for the Examination of Water and Wastewater (3500 Fe-B method) [44] and Nogueira et al. [45] respectively.

The composition of the material (Si, Al, and Fe) was determined by X-ray fluorescence (MiniPaI4–PANalytical); iron speciation in the catalyst was determined by diffuse reflectance (UV 3600–Shimadzu); and crystallinity by X-ray diffraction (D8 Advance–Bruker). In addition, the specific surface areas were determined by N_2 adsorption/desorption (ASAP 2020–Micromeritics).

3. Results and discussion

3.1. Catalyst characterization

The determination of the main elements that constituted the natural zeolite, before and after the modification processes, was performed by X-ray fluorescence. It was possible to follow the most important changes in these materials, for example, the SiO_2/Al_2O_3 ratio and the iron concentration (Fig. 4).

The SiO_2/Al_2O_3 ratio is an important parameter whenever aluminosilicates are used as support materials for catalysts. This ratio shows the hydrophobicity of the material [46], affecting the mechanism and efficiency of the reaction by changing the affinity between the organic compound and the catalyst. It was possible to observe that the treatment steps with HCl increased almost 3 times the value of the SiO_2/Al_2O_3 ratio (from 9 to 26), making the treated zeolite more hydrophobic. However, the acid treatments, in addition to removing aluminum [47], also removed most of the iron originally present in the material (2.6% in mass). Therefore, iron needed to be added to the zeolite, generating a material with 1.4% of Fe. The reintroduction of Fe did not affect the hydrophobicity of the catalyst.

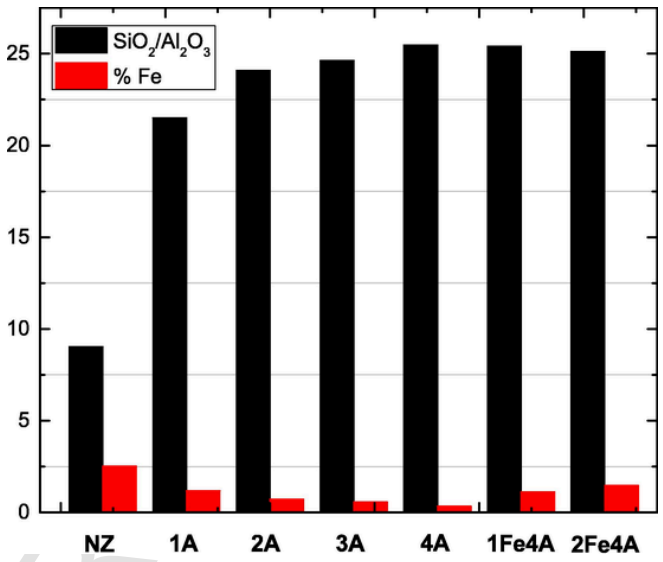

Fig. 4. Composition of the natural zeolite (NZ) and the materials obtained after the modification processes. A = 1 mol L^{-1} HCl treatment; Fe = iron impregnation treatment. Numbers represent how many times each treatment was performed.

In addition to increasing the SiO_2/Al_2O_3 ratio, the acid treatments also removed much of the impurities present in the natural zeolite. During such treatments, the zeolitic channels were unblocked, contributing to the addition of higher amounts of iron and the significant increase in the specific surface area of the material (Fig. 5).

It was decided to determine the iron speciation of the material, as the catalytic activity is related to different H_2O_2 decomposition mechanisms, whether free iron or iron oxides are present [48]. The synthesized samples were ground to a powder, which was analyzed by diffuse reflectance (Fig. 6).

The bands below 300 nm represent the mono and binuclear Fe(III) species, which are responsible for the most efficient hydroxyl radical

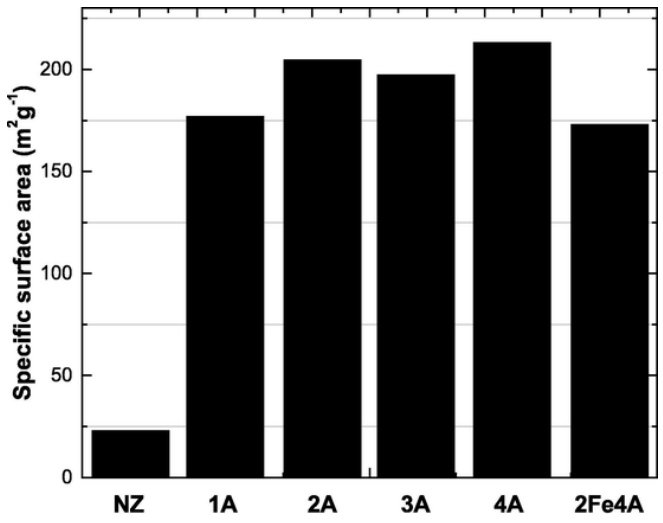

Fig. 5. Specific surface area of the materials during the synthetic steps of the catalyst. NZ = natural zeolite. 1A = first acid treatment (1 mol L^{-1} HCl); 2Fe = second (Fe addition) treatment. Numbers represent how many times each treatment was performed.

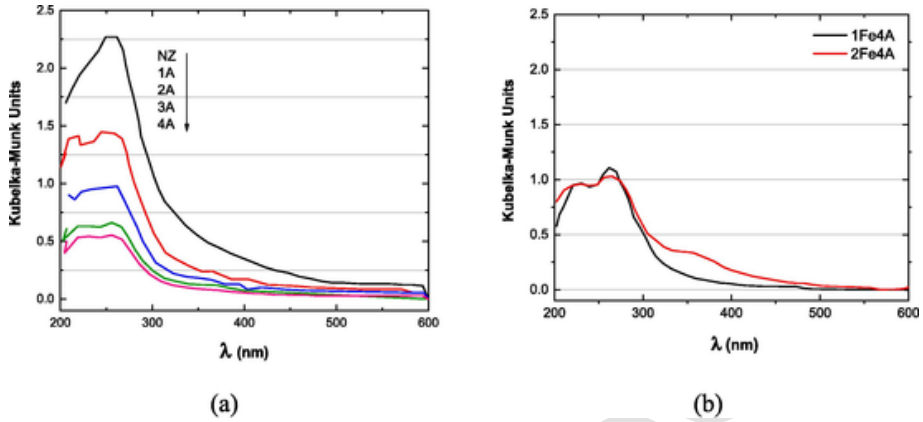

Fig. 6. Diffuse reflectance spectra of the synthesized materials: (a) acid and (b) Fe impregnation treatments.

production. The bands above 300 nm are due to the presence of iron oxides [49]. Although the natural zeolite iron concentration was greater than the one obtained in the catalyst (2Fe4A), this "extra" iron was not available for decomposing hydrogen peroxide, due to the low specific surface area, that is, the zeolitic channels were blocked, preventing H_2O_2 diffusion. It was observed that the increase of the available space inside the zeolite also had a negative side: it allowed the formation of iron oxides, as observed in Fig. 6b.

The dealumination steps (HCl treatment) were also monitored by X-ray diffraction (Fig. 7). As the natural zeolite had several impurities, its diffractogram was composed of multiple peaks, but it was possible to observe the characteristic peaks of heulandite, which makes up 70% of the material. During dealumination, such peaks stand out, and after four cycles of HCl treatment, a characteristic peak of quartz was observed. Therefore, one can observe that after the acid treatment, heulandite remained as the main mineral present in the catalyst.

3.2. Batch degradation experiments

In the characterization step of the materials, it was found that: (a) NZ, 1A, and 2Fe4A materials contained mono and binuclear Fe(III) and (b) 1A and 2Fe4A materials had specific surface areas around 180 m^2 g^{-1}. Therefore, it was decided to determine the catalytic activity of these materials towards the decomposition of H_2O_2 (Fig. 8). Open flasks containing suspensions of the materials (10 g L^{-1}, each) in biologically treated sewage and 2 g L^{-1} H_2O_2, all at pH 7.3 ± 0.2, were magnetically stirred for 8 h at room temperature (22 ± 2 °C).

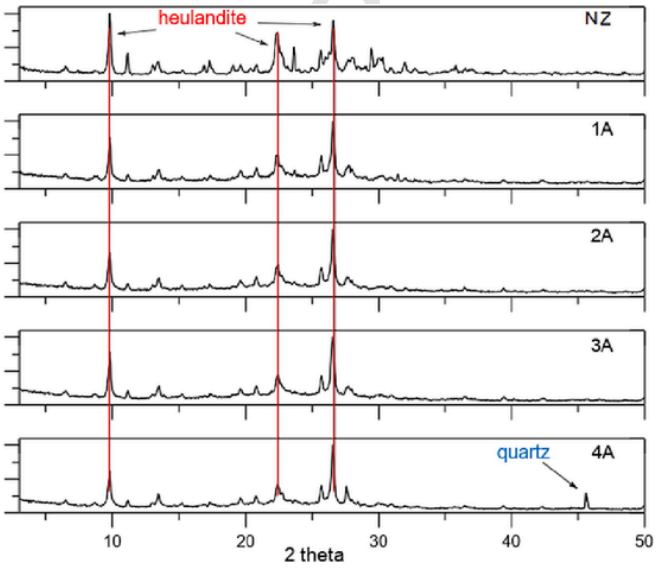

Fig. 7. X-ray diffractograms of the natural zeolite (NZ) and the respective materials obtained during the dealumination steps.

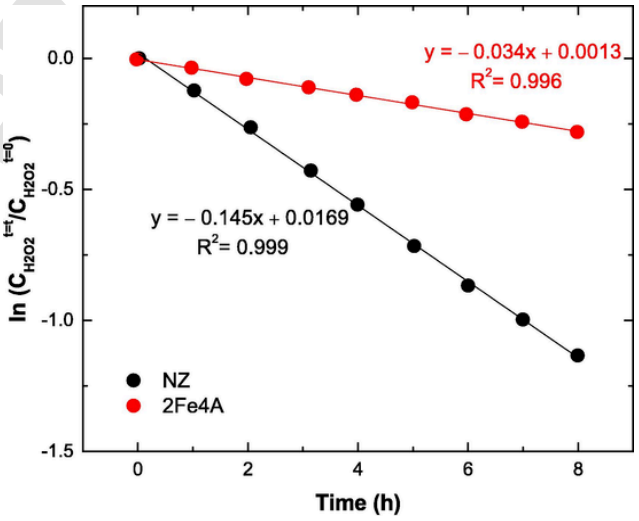

Fig. 8. Hydrogen peroxide decomposition in suspensions of natural zeolite (NZ) and modified zeolite (2Fe4A): $C_{H_2O_2}$ = 2 g L^{-1}, C_{2Fe4A} = 10 g L^{-1}, and pH = 7.3 ± 0.2.

A set of initial experiments (not shown here) were performed to obtain a H_2O_2 concentration in which significant degradation was achieved: 2 g L^{-1} was the smallest concentration that fulfilled that purpose.

The natural zeolite subjected to one acid treatment step (1A) did not decompose H_2O_2, even after 20 h of reaction. Although 1A had 1.12% Fe, the active sites for the reaction with hydrogen peroxide appeared to be inactivated. Therefore, this material was not used in the following experiments.

In relation to the other two catalysts, NZ and 2Fe4A, it was observed that the H_2O_2 decomposition followed a pseudo-first order kinetics, $\ln(C^{t=t}_{H_2O_2}/C^{t=0}_{H_2O_2}) = -k_{H_2O_2}t$. Then, the catalytic activity ($A_{H_2O_2}$ in L $g^{-1}h^{-1}$) was calculated for each material (Equation (1), in which $k_{H_2O_2}$ is the pseudo-first order degradation rate constant (h^{-1}) and C_{cat} is the concentration of the catalyst (g L^{-1}).

$$A_{H_2O_2} = \frac{k_{H_2O_2}}{C_{cat}} \quad (1)$$

The calculated $A_{H_2O_2}$ were 3.40×10^{-3} and 1.45×10^{-2} L $g^{-1}h^{-1}$ for 2Fe4A and NZ, respectively. Although the NZ catalytic activity for the decomposition of H_2O_2 was approximately four times greater than the one of 2Fe4A, one cannot state that this material is the best catalyst for degrading the drugs. Hydroxyl radical reactions preferentially occur inside the zeolitic channels [39] and perhaps NZ only allowed for the diffusion of small molecules, like H_2O_2. Therefore, experiments were performed with NZ and 2Fe4A to check the degradation of the drugs.

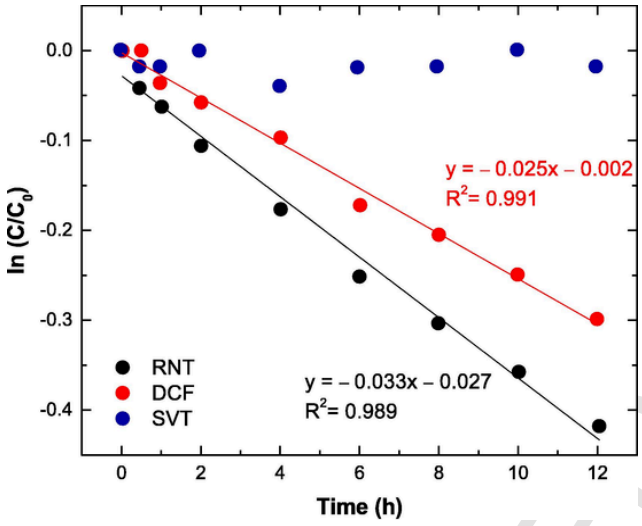

Fig. 9. Degradation of diclofenac (DCF), ranitidine (RNT), and simvastatin (SVT) by the heterogeneous Fenton process using the 2Fe4A catalyst (C_{drugs} = 50 μg L^{-1}, each; $C_{H_2O_2}$ = 2 g L^{-1}; $C_{catalyst}$ = 10 g L^{-1}; and pH 7.3 ± 0.2).

A solution containing the drugs mixture (DCF, RNT, and SVT, 50 μg L^{-1} each) was prepared with biologically treated sewage. This solution was used to prepare 10 g L^{-1} of NZ and 2Fe4A suspensions, to which H_2O_2 2 g L^{-1} was added. The experiments were performed under stirring for 12 h. Assays without H_2O_2 were also performed to verify the contribution of adsorption. Nevertheless, drugs degradation was only observed in the presence of the 2Fe4A catalyst (Fig. 9). That is probably because unblocking the zeolite channels is mandatory to achieve significant degradation.

Only 2% of DCF was removed by adsorption in the experiments with 2Fe4A; the removal of the other drugs was not affected by this process. It was concluded that NZ had less accessible cavities because only hydrogen peroxide could be degraded.

SVT degradation was possibly affected by its molecular size, which is a limiting factor in the case of the heterogeneous Fenton process using zeolites as a support (Fig. 10). This size exclusion effect was less significant for RNT and DCF because both have at least one dimension compatible (Fig. 10) with zeolite channel entries, which in the case of heulandite is up to 7.5 Å. RNT and DCF degradation occurred with a pseudo-first order kinetics and Equation (1) could be used to calculate the respective catalytic activities: 3.3×10^{-3} and 2.5×10^{-3} L $g^{-1}h^{-1}$. No DOC removal was observed in any of these experiments.

In order to check the effect of the homogeneous process, the liquid phase was separated from the respective catalysts by centrifugation, and maintained in the experimental conditions for another 12 h. It was found that the degradation of the drugs was exclusively due to the heterogeneous process. The liquid phase was subjected to total iron analysis and it was found that only 1.1 ± 0.2% of the initial concentration supported on the zeolite was leached.

The dissolution of the iron supported on the zeolite would have a direct negative effect on the catalytic activity, as this element would be gradually removed from the reactor. To check the 2Fe4A resistance to iron leaching, oxalate was added to the degradation system (the suspension prepared with biologically treated sewage containing the drugs, hydrogen peroxide, and the catalyst). That anion is a small and strong

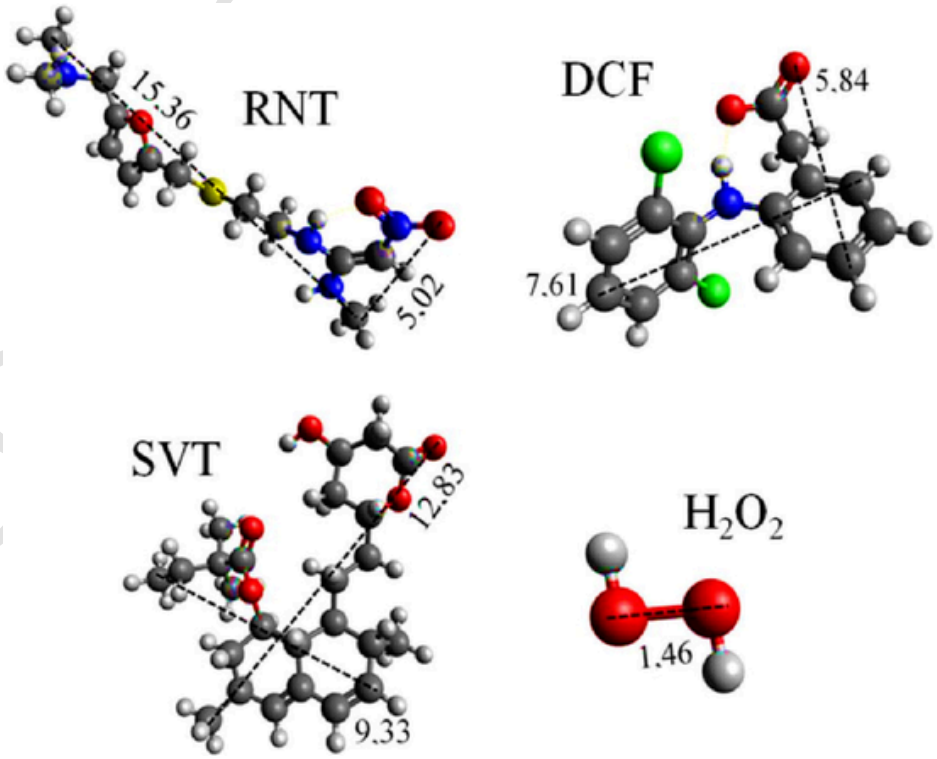

Fig. 10. Ranitidine (RNT), diclofenac (DCF), simvastatin (SVT), and hydrogen peroxide (H_2O_2) dimensions (Å). 3D-geometry obtained using the Avogadro software (MMFF94-force field).

iron complexing agent. This experiment was performed in 5 cycles of 30 h each, using RNT as the model-compound. After separating the zeolite by centrifugation at the end of each cycle, the solution containing the drugs, hydrogen peroxide, and oxalate was renewed, that is, the zeolite was reused (Fig. 11). Considering that the iron mass fraction in 2Fe4A is 1.4%, oxalate was added at a molar concentration 3 times higher. Prior to iron quantification, samples were digested to avoid oxalate interference in color formation.

The experiments in the presence of oxalate showed that the iron dissolution is more significant in the first two cycles; from the third cycle on leaching was < 0.1% of the amount of total iron in the reaction system. This test was important because it showed that the catalyst would be resistant at continuous operation of the reactor when combined to the biological process. It was also observed that the degradation of RNT was impaired neither by the dissolution of iron nor by the presence of oxalate, as $k_{HO\bullet,oxalate} = 1.4 \times 10^{-6}$ L mol^{-1} s^{-1} [50].

3.3. Continuous degradation experiments

Considering that both hydrogen peroxide and drugs degradations followed pseudo-first order kinetics, Equation (2) was used to estimate the conditions of the fixed-bed reactor. It was estimated that to obtain 90% of DCF degradation, the HRT would be 12 min.

$$\ln \frac{C}{C_0} = -A.C_{cat}.t \quad (2)$$

Hydrodynamic tests, for determining the average HRT, were carried out before the degradation experiments. In this way, it was possible to determine the appropriate flow rates according to the results obtained in the batch experiments. Figure S1 shows the curve obtained in the tests.

The step curve observed for the fixed-bed reactor is characteristic of plug-flow reactors (PFR). The filling granulometry and the reactor internal diameter contributed to this behavior. The reactor flow rate was 0.7 mL min^{-1}, so that the average HRT was 12 min.

DCF was used as a reference because this compound showed the lowest degradation rate in the batch tests, that is, if DCF is completely degraded, RNT would probably be too. At this stage, SVT was not monitored, as it was not degraded by the heterogeneous Fenton process using 2Fe4A as the catalyst. Fig. 12 shows the stability of the process during 10 days of continuous operation.

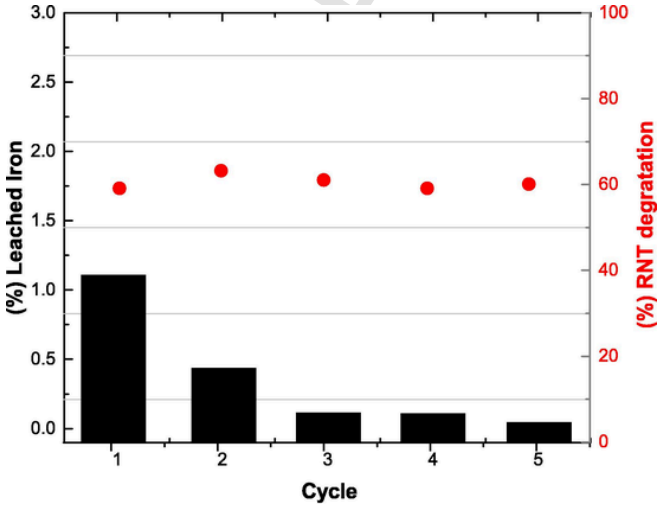

Fig. 11. Total iron leached from 2Fe4A after cycles of 30 h in the presence of oxalate at a molar ratio of 1:3 (Fe:oxalate). Effect of iron dissolution on ranitidine (RNT) degradation.

Fig. 12 shows that the heterogeneous Fenton process was efficient for the degradation of DCF and RNT, as the fractions of these contaminants at the output of the reactor were 18 and 2% of the initial concentration of the drugs, respectively. It is also noted that this process was somewhat selective, as no COD removal was observed, which means that no mineralization was observed. It is possible to observe that, under the studied conditions, DCF degradation was less than the one obtained in the batch tests. This may have occurred due to the particle size increase (from < 75 to 300–500 μm), which impaired mass transfer. Under the experimental conditions, approximately 93% of the H_2O_2 was consumed and the DP-DCF (diclofenac degradation product), identified by Silva et al. (2020) [40] during the operation of the anaerobic–aerobic reactor), was not detected at the heterogeneous Fenton reactor outlet.

An alternative for reducing the cost of the process and increasing drugs degradation would be to reduce the initial concentration of hydrogen peroxide, as this oxidant can compete with the drugs for the hydroxyl radical (Equation (3) [51].

$$H_2O_2 + OH^{\cdot} \rightarrow HO_2^{\cdot} + H_2O \quad (3)$$

This strategy was adopted, and the hydrogen peroxide initial concentration was changed from 2 to 1 g L^{-1} and the reactor was operated for two days. It was observed that approximately the same amount of hydrogen peroxide was consumed (considering the batch tests). On the other hand, the drugs degradation was significantly affected (decreased) and removal efficiencies were 55 and 83% for DCF and RNT, respectively. Therefore, it seemed that this process required a minimum concentration of hydrogen peroxide in the bed, so that the drugs were efficiently degraded, and such concentration was close to 2 g L^{-1}.

3.4. Cost estimate of the heterogeneous Fenton process

Considering the average per capita production of domestic sewage, that is, 160 L day^{-1} cap^{-1} [52], the operating cost of the heterogeneous Fenton process was estimated for obtaining 90% drugs degradation in the domestic sewage produced by 2,000 inhabitants. It is important to emphasize that the estimated values are for that process after an anaerobic–aerobic treatment.

For HRT = 12 min, $C_{H_2O_2}$ = 2 g L^{-1}, and 55% porosity (catalyst in pellets), the reactor total volume would be 4.85 m^3. Therefore, 3,976 kg of natural zeolite (US$ 0.05 kg^{-1}) [53] would be needed, whose cost is US$ 198.79. It was estimated that 2.2 kg HCl and 0.39 kg $FeSO_4{\cdot}7H_2O$ kg^{-1} NZ are needed for the synthesis of the 2Fe4A catalyst; those chemicals cost US$ 0.55 kg^{-1} and US$ 0.13 kg^{-1} [54], respectively. Therefore, the catalyst cost would be US$ 5012.24. Only the consumption of hydrogen peroxide (2 kg m^{-3}) was considered (US$ 0.66 kg^{-1}): US$ 1.32 m^{-3}. A detailed "Calculation Report" is given in the Supplementary material.

4. Conclusions

Natural zeolite (70% heulandite, 15% anorthite, 10% quartz, and 5% mordenite), once purified (acid treatment) and impregnated with iron, proved to be a suitable catalyst for removing diclofenac and ranitidine by the heterogeneous Fenton process from a biologically-treated domestic sewage. Besides removing impurities, the acid treatment unblocked zeolite channels and increased its hydrophobicity (SiO_2/Al_2O_3 ratio). However, simvastatin could not be degraded. That is probably because simvastatin, due to its dimensions, was not able to diffuse into the zeolite channels.

The modified zeolite was quite stable, maintaining its degradation performance in batch mode for five cycles of 30 h each, with low iron leaching. Likewise, the performance of the herein proposed continuous coupled system was stable for, at least, 10 days.

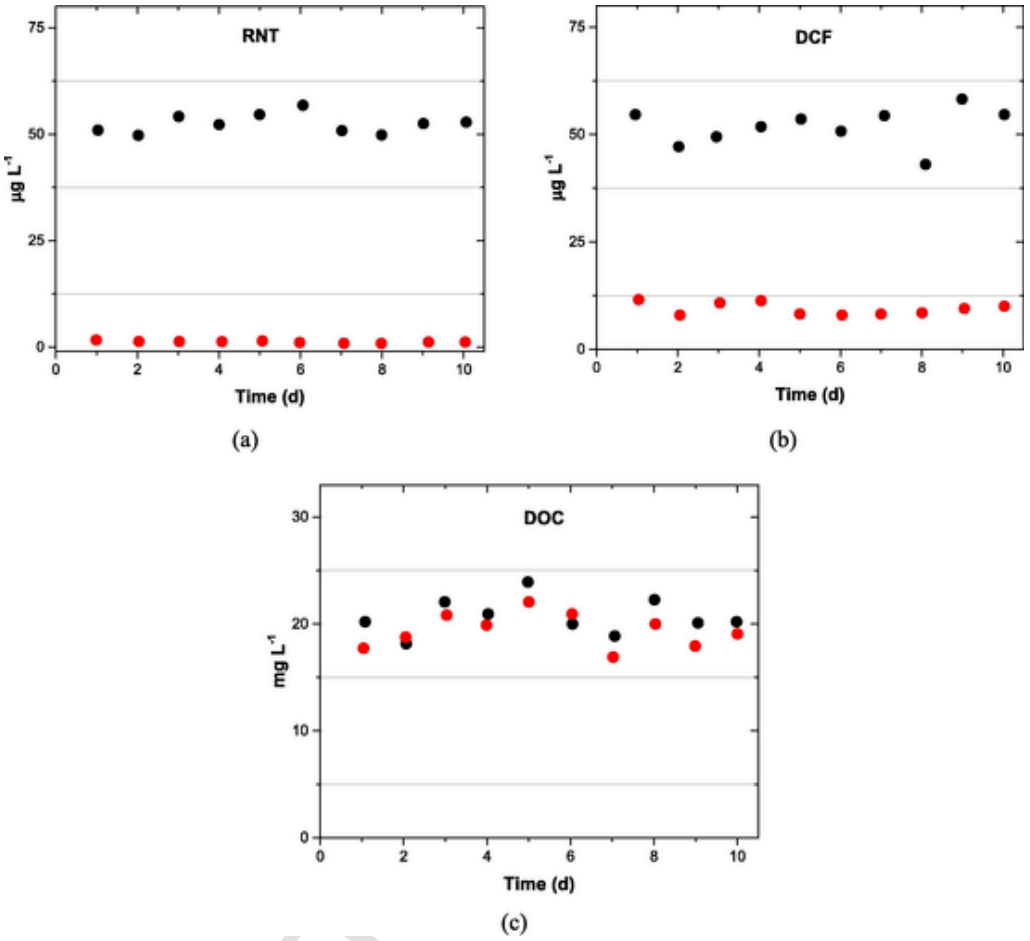

Fig. 12. (a) Ranitidine (RNT), (b) dicoflenac (DCF) degradations, and (c) residual dissolved organic carbon (DOC) by the heterogeneous Fenton process combined to the anaerobic–aerobic process: (●) Input and (●) Output.

The main disadvantages of the system were a relatively high consumption of hydrogen peroxide, size exclusion effects, and the absence of observable mineralization, maybe due to the small hydraulic retention time (12 min).

Declaration of Competing Interest

The authors declare that they have no known competing financial interests or personal relationships that could have appeared to influence the work reported in this paper.

Data availability

Data will be made available on request.

Acknowledgments

This work was supported by the São Paulo Research Foundation (FAPESP) [2009/53850-6, 2012/09569-3, 2014/04550-8]; and Coordenação de Aperfeiçoamento de Pessoal de Nível Superior – Brasil (CAPES) – Finance Code 001.

Appendix A. Supplementary data

Supplementary data to this article can be found online at https://doi.org/10.1016/j.cej.2023.143509.

References

[1] Y. Jeong, A. Schäffer, K.A. Smith, Comparison of equilibrium and kinetic passive sampling for the monitoring of aquatic organic contaminants in German rivers, Water Res. 145 (2018) 248–258, https://doi.org/10.1016/j.watres.2018.08.016.
[2] O.F.S. Khasawneh, P. Palaniandy, Occurrence and removal of pharmaceuticals in wastewater treatment plants, Process Saf. Environ. 150 (2021) 532–556, https://doi.org/10.1016/j.psep.2021.04.045.
[3] S. Silvestri, C.D. Ferreira, V. Oliveira, J.M.T.B. Varejão, J.A. Labrincha, D.M. Tobaldi, Synthesis of PPy-ZnO composite used as photocatalyst for the degradation of diclofenac under simulated solar irradiation, J. Photochem. Photobio. A 375 (2019) 261–269, https://doi.org/10.1016/j.jphotochem.2019.02.034.
[4] J.C.G. Sousa, A.R. Ribeiro, M.O. Barbosa, C. Ribeiro, M.E. Tiritan, M.F.R. Pereira, A.M.T. Silva, Monitoring of the 17 EU Watch List contaminants of emerging concern in the Ave and the Sousa Rivers, Sci. Total Environ. 649 (2019) 1083–1095, https://doi.org/10.1016/j.scitotenv.2018.08.309.
[5] D. Bojić, M. Momčilović, D. Milenković, J. Mitrović, P. Banković, N. Velinov, G. Nikolić, Characterization of a low cost Lagenaria vulgaris based carbon for ranitidine removal from aqueous solutions, Arab. J. Chem. 10 (2017) 956–964, https://doi.org/10.1016/j.arabjc.2014.12.018.
[6] K. Czerniak, J. Cielecka-Piontek, P. Zalewski, Ultra fast HPLC method for determination of ranitidine hydrochloride using a core-shell column, Acta Pol. Pharm. 74 (2017) 1637–1643.
[7] E. Mugunthan, M.B. Saidutta, P.E. Jagadeeshbabu, Photocatalytic degradation of diclofenac using TiO 2 –SnO 2 mixed oxide catalysts, Environ. Technol. 40 (7) (2019) 929–941.
[8] M. Rostamizadeh, H. Jalali, F. Naeimzadeh, S. Gharibian, Efficient removal of diclofenac from pharmaceutical wastewater using impregnated zeolite catalyst in heterogeneous Fenton process, Phys. Chem. Res. 7 (2019) 37-52. https://doi.org/10.22036/pcr.2018.144779.1524.
[9] M. Hadzieva Gigovska, A. Petkovska, J. Acevska, N. Nakov, P. Antovska, S. Ugarkovic, A. Dimitrovska, Comprehensive Assessment of Degradation Behavior of Simvastatin by UHPLC/MS Method, Employing Experimental Design Methodology, Int. J. Anal. Chem. 2018 (2018) 1–17.
[10] A.D.T. Liyanage, A.J. Chen, D.A. Puleo, Biodegradable simvastatin-containing

polymeric prodrugs with improved drug release, ACS Biomater. Sci. Eng. 4 (2018) 4193–4199, https://doi.org/10.1021/acsbiomaterials.8b00884.
[11] Z.H. Mussa, F.F. Al-Qaim, M.R. Othman, M.P. Abdullah, Removal of simvastatin from aqueous solution by electrochemical process using graphite-PVC as anode: A case study of evaluation the toxicity, kinetics and chlorinated by-products, J. Environ. Chem. Eng. 4 (2016) 3338–3347, https://doi.org/10.1016/j.jece.2016.07.006.
[12] M.S. Shamsudin, S.F. Azha, S. Ismail, A review of diclofenac occurrences, toxicology, and potential adsorption of clay-based materials with surfactant modifier, J. Environ Chem. Eng. 10 (3) (2022) 107541.
[13] M. Patel, R. Kumar, K. Kishor, T. Mlsna, C.U. Pittman Jr, D. Mohan, Pharmaceuticals of emerging concern in aquatic systems: chemistry, occurrence, effects, and removal methods, Chem. Rev. 119 (2019) 3510–3673, https://doi.org/10.1021/acs.chemrev.8b00299.
[14] V.S. Tete, H. Nyoni, B.B. Mamba, T.A.M. Msagati, Occurrence and spatial distribution of statins, fibrates and their metabolites in aquatic environments, Arab. J. Chem. 13 (2020) 4358–4373, https://doi.org/10.1016/j.arabjc.2019.08.003.
[15] S.K. Alharbi, L.D. Nghiem, J.P. van de Merwe, F.D.L. Leusch, M.B. Asif, F.I. Hai, W.E. Price, Degradation of diclofenac, trimethoprim, carbamazepine, and sulfamethoxazole by laccase from Trametes versicolor: Transformation products and toxicity of treated effluent, Biocatal. Biotransfor. 10 (2019) 399–408, https://doi.org/10.1080/10242422.2019.1580268.
[16] X. Quan, X. Wang, Y. Sun, W. Li, L. Chen, J. Zhao, Degradation of diclofenac using palladized anaerobic granular sludge: Effects of electron donor, reaction medium and deactivation factors, J. Hazard. Mater. 365 (2019) 155–163, https://doi.org/10.1016/j.jhazmat.2018.10.100.
[17] A.S. Adeleye, J. Xue, Y. Zhao, A.A.Y. Taylor, A.A. Zenobio, J.E. Sun, Z. Han, O.A. Salawu, Y. Zhu, Abundance, fate, and effects of pharmaceuticals and personal care products in aquatic environments, J. Hazard. Mater. 424 (2022) 127284, https://doi.org/10.1016/j.jhazmat.2021.127284.
[18] A.S. Richey, B.F. Thomas, M.-H. Lo, J.T. Reager, J.S. Famiglietti, K. Voss, S. Swenson, M. Rodell, Quantifying renewable groundwater stress with GRACE, Water Resour. Res. 51 (2015) 5217–5238, https://doi.org/10.1002/2015WR017349.
[19] A.C. Petrasek, I.J. Kugelman, B.M. Austern, B.M. Pressley, L.A. Winslow, R. Wise, Fate of toxic organic compounds in wastewater treatment plants, J. Water Pollut. Con. F. 55 (1983) 1286–1296.
[20] H. Demir-Duz, O. Ayyildiz, A.S. Aktürk, M.G. Álvarez, S. Contreras, Approaching zero discharge concept in refineries by solar–assisted photo-Fenton and photo-catalysis processes, Appl. Catal. B-Environ. 248 (2019) 341–348, https://doi.org/10.1016/j.apcatb.2019.02.026.
[21] M.M.H. Guerra, I.A. Oller, S.M. Rodriguez, A.A. López, A.A. Merino, J.M.A. Alonso, Oxidation mechanisms of amoxicillin and paracetamol in the photo-Fenton solar process, Water Res. 156 (2019) 232–240, https://doi.org/10.1016/j.watres.2019.02.055.
[22] M.P. Rayaroth, C.T. Aravindakumar, N.S. Shah, G. Boczkaj, Advanced oxidation processes (AOPs) based wastewater treatment - unexpected nitration side reactions - a serious environmental issue: A review, Chem. Eng. J. 430 (2022) 133002, https://doi.org/10.1016/j.cej.2021.133002.
[23] F.S. Souza, L.A. Feris, Degradation of caffeine by advanced oxidative processes: O-3 and O-3/UV, Ozone-Sci. Eng. 37 (2015) 379–384, https://doi.org/10.1080/01919512.2015.1016572.
[24] Y. Ma, H. Wang, X. Lv, D. Xiong, H. Xie, Z. Zhang, Three-dimensional ordered mesoporous Co_3O_4/peroxymonosulfate triggered nanoconfined heterogeneous catalysis for rapid removal of ranitidine in aqueous solution, Chem. Eng. J. 443 (2022) 136495, https://doi.org/10.1016/j.cej.2022.136495.
[25] K.O. Rahman, K.H.H. Aziz, Utilizing scrap printed circuit boards to fabricate efficient Fenton-like catalysts for the removal of pharmaceutical diclofenac and ibuprofen from water, J. Environ. Chem. Eng. 10 (6) (2022) 109015, https://doi.org/10.1016/j.jece.2022.109015.
[26] I. Lozano, C.J. Pérez-Guzmán, A. Mora, J. Mahlknecht, C.L. Aguilar, P. Cervantes-Avilés, Pharmaceuticals and personal care products in water streams: Occurrence, detection, and removal by electrochemical advanced oxidation processes, Sci. Total Environ. 827 (2022) 154348, https://doi.org/10.1016/j.scitotenv.2022.154348.
[27] C. Christophoridis, M.-C. Nika, R. Aalizadeh, N.S. Thomaidis, Ozonation of ranitidine: Effect of experimental parameters and identification of transformation products, Sci. Total Environ. 557–558 (2016) 170–182, https://doi.org/10.1016/j.scitotenv.2016.03.026.
[28] H. Olvera-Vargas, N. Oturan, M.A. Oturan, E. Brillas, Electro-Fenton and solar photoelectro-Fenton treatments of the pharmaceutical ranitidine in pre-pilot flow plant scale, Separation Purification Technol. 146 (2015) 127–135.
[29] K.V. Plakas, A. Mantza, S.D. Sklari, V.T. Zaspalis, A.J. Karabelas, Heterogeneous Fenton-like oxidation of pharmaceutical diclofenac by a catalytic iron-oxide ceramic microfiltration membrane, Chem. Eng. J. 373 (2019) 700–708, https://doi.org/10.1016/j.cej.2019.05.092.
[30] M. Anis, S. Haydar, Heterogeneous Fenton oxidation of caffeine using zeolite-supported iron nanoparticles, Arab. J. Sci. Eng. 44 (2019) 315–328, https://doi.org/10.1007/s13369-018-3659-3.
[31] J.A. Botas, J.A. Melero, F. Martínez, M.I. Pariente, Assessment of Fe_2O_3/SiO_2 catalysts for the continuous treatment of phenol aqueous solutions in a fixed bed reactor, Catal. Today 149 (2010) 334–340, https://doi.org/10.1016/j.cattod.2009.06.014.
[32] A. Cabrera Reina, S. Miralles-Cuevas, J.L. Casas López, J.A. Sánchez Pérez, Pyrimethanil degradation by photo-Fenton process: Influence of iron and irradiance level on treatment cost, Sci. Total Environ. 605–606 (2017) 230–237, https://doi.org/10.1016/j.scitotenv.2017.06.217.
[33] A. Georgi, R. Gonzalez-Olmos, R. Köhler, F.-D. Kopinke, Fe-zeolites as catalysts for wet peroxide oxidation of organic groundwater contaminants: mechanistic studies and applicability tests, Sep. Sci. Techno. 45 (2010) 1579–1586, https://doi.org/10.1080/01496395.2010.487466.
[34] J. He, X. Yang, B. Men, D. Wang, Interfacial mechanisms of heterogeneous Fenton reactions catalyzed by iron-based materials: A review, J. Environ. Sci. 39 (2016) 97–109, https://doi.org/10.1016/j.jes.2015.12.003.
[35] A.I. Zárate-Guzmán, L.V. González-Gutiérrez, L.A. Godínez, A. Medel-Reyes, F. Carrasco-Marín, L.A. Romero-Cano, Towards understanding of heterogeneous Fenton reaction using carbon-Fe catalysts coupled to in-situ H_2O_2 electro-generation as clean technology for wastewater treatment, Chemosphere 224 (2019) 698–706, https://doi.org/10.1016/j.chemosphere.2019.02.101.
[36] S. Navalon, A. Dhakshinamoorthy, M. Alvaro, H. Garcia, Heterogeneous Fenton catalysts based on activated carbon and related materials, ChemSusChem 4 (12) (2011) 1712–1730, https://doi.org/10.1002/cssc.201100216.
[37] N. Nasseh, L. Taghavi, B. Barikbin, M.A. Nasseri, A. Allahresani, $FeNi_3/SiO_2$ magnetic nanocomposite as an efficient and recyclable heterogeneous fenton-like catalyst for the oxidation of metronidazole in neutral environments: Adsorption and degradation studies, Compos. Part B-Eng. 166 (2019) 328–340, https://doi.org/10.1016/j.compositesb.2018.11.112.
[38] Z. Shangguan, X. Yuan, C. Qin, Y. Zhao, H. Chen, X. Zheng, J. Wu, J. Guo, H. Wang, Improving the removal of tetracycline via carbonate-mediated triplet-excited state by the Cu-containing zeolites activated percarbonate, Chem. Eng. J. 457 (2023) 141046, https://doi.org/10.1016/j.cej.2022.141046.
[39] S. Caudo, G. Centi, C. Genovese, S. Perathoner, Homogeneous versus heterogeneous catalytic reactions to eliminate organics from waste water using H_2O_2, Top Catal. 40 (1–4) (2006) 207–219.
[40] T.H.G. Silva, R.X.S. Furtado, M. Zaiat, E.B. Azevedo, Tandem anaerobic-aerobic degradation of ranitidine, diclofenac, and simvastatin in domestic sewage, Sci. Total Environ. 721 (2020) 137589, https://doi.org/10.1016/j.scitotenv.2020.137589.
[41] D. Verboekend, T.C. Keller, M. Milina, R. Hauert, J. Perez-Ramirez, Hierarchy brings function: Mesoporous clinoptilolite and L zeolite catalysts synthesized by tandem acid-base treatments, Chem. Mater. 25 (2013) 1947–1959, https://doi.org/10.1021/cm4006103.
[42] R. Althoff, A. Tissler, H. Toufar, Metal doped zeolite and process for its preparation, Google Patents (2010).
[43] O. Levenspiel, Chemical Reaction Engineering, third ed, John Wiley and Sons, New York, 1999.
[44] American Public Health Association (APHA), American Water Works Association (AWWA),Water Environmental Federation (WEF), Standard Methods for the Examination of Water and Wastewater, twenty-first ed, American Public Health Association, Washington, 2005.
[45] R. Nogueira, M. Oliveira, W. Paterlini, Simple and fast spectrophotometric determination of H_2O_2 in photo-Fenton reactions using metavanadate, Talanta 66 (1) (2005) 86–91.
[46] C. Wang, H. Guo, S. Leng, J. Yu, K. Feng, L. Cao, J. Huang, Regulation of hydrophilicity/hydrophobicity of aluminosilicate zeolites: a review, Critical Rev. Solid State Mater. Sci. 46 (4) (2021) 330–348.
[47] C. Wang, S. Leng, H. Guo, L. Cao, J. Huang, Acid and alkali treatments for regulation of hydrophilicity/hydrophobicity of natural zeolite, Appl. Surf. Sci. 478 (2019) 319–326, https://doi.org/10.1016/j.apsusc.2019.01.263.
[48] F. Araujo, L. Yokoyama, L. Teixeira, J. Campos, Heterogeneous Fenton process using the mineral hematite for the discolouration of a reactive dye solution, Braz. J. Chem. Eng. 28 (2011) 605-616. https://doi.org/ 10.1590/S0104-66322011000400006.
[49] R. Gonzalez-Olmos, F.D. Kopinke, K. Mackenzie, A. Georgi, Hydrophobic Fe-zeolites for removal of MTBE from water by combination of adsorption and oxidation, Environ. Sci. Technol. 47 (2013) 2353–2360, https://doi.org/10.1021/es303885y.
[50] B.A. Wols, C.H.M. Hofman-Caris, Review of photochemical reaction constants of organic micropollutants required for UV advanced oxidation processes in water, Water Res. 46 (2012) 2815–2827, https://doi.org/10.1016/j.watres.2012.03.036.
[51] J.J. Pignatello, E. Oliveros, A. MacKay, Advanced Oxidation Processes for Organic Contaminant Destruction Based on the Fenton Reaction and Related Chemistry, Critical Rev. Environ. Sci. Technol. 36 (1) (2006) 1–84.
[52] Metcalf, Eddy, Wastewater Engineering: Treatment and Reuse, fourth ed, McGraw-Hill, New York, 2003.
[53] N. Eroglu, M. Emekci, C.G. Athanassiou, Applications of natural zeolites on agriculture and food production, J. Sci. Food Agr. 97 (2017) 3487–3499, https://doi.org/10.1002/jsfa.8312.
[54] Kemcore, Mining chemicals and services. http://www.kemcore.com, 2022 (acessed 2 November 2022).